NUMERICAL SIMULATION OF O_2/CO_2 COMBUSTION IN DECOMPOSITION FURNACE

by

Bo WANG and Hongtao KAO*

College of Materials Science and Engineering, Nanjing Tech University, Nanjing, China

Original scientific paper
https://doi.org/10.2298/TSCI221217073W

The cement industry has become the second largest source of CO_2 and NO_x emissions after the power industry, it is imperative to reduce CO_2 and NO_x emissions. O_2/CO_2 combustion technology can achieve CO_2 enrichment and NO_x reduction. As a result, its application possibilities are bright. In this article, a TTF-type decomposition furnace serves as the research object for a CFD simulation. In addition, the effects of pulverized coal combined O_2/N_2 and pulverized coal mixed O_2/CO_2 combustion on the velocity field, temperature field, material component, and NO_x concentration distribution in the furnace are investigated concerning the changes of kinetic parameters of $CaCO_3$ decomposition under different working conditions. Compared with the O_2/N_2 atmosphere, the temperature distribution in the high temperature zone of the decomposition furnace is more uniform under the O_2/CO_2 atmosphere. The temperature range is reduced in the area of extremely high temperatures. The NO_x concentration at the decomposition furnace exit is reduced by 37%. The high concentration of CO_2 at the output can be recycled and reused to reduce the greenhouse effect effectively. In addition, the high CO_2 partial pressure increases the exit temperature by 111 K, doubles the O_2 concentration, but decreases the raw meal decomposition rate from 95.9-82.2%. The process parameters must be improved to adapt to the O_2/CO_2 combustion technology.

Key words: *O_2/CO_2 combustion, CO_2 emission reduction, numerical simulation*

Introduction

With the rapid growth of global energy demand, the use of fossil fuels has led to an increase in CO_2 emissions and a worsening of the greenhouse effect. Therefore, the reduction of CO_2 emissions has become an important research field. As the second largest source of CO_2 emission after the electric power industry [1], the cement industry has great potential to reduce CO_2 emissions. The most promising development technology to achieve CO_2 emission reduction in the cement industry is CO_2 capture technology. In order to achieve CO_2 capture, CO_2 must be separated directly from the flue gas, and the difficulty and cost of standard capture technology are significant. Therefore, O_2/CO_2 combustion technology was born and has attracted more and more attention [2, 3].

Cement kiln O_2/CO_2 combustion technology is to mix high purity O_2 (>95%) with circulating flue gas and passes it into the decomposition furnace and rotary kiln for combustion so that pulverized coal combustion is burned in the O_2/CO_2 atmosphere. After multiple enrichment, the CO_2 gas in the kiln tail has high purity and can be directly recycled, stored, and utilized. Also, CO_2 has higher heat and mass transfer characteristics than N_2, which can

* Corresponding author, e-mail: kaoht@163.com

improve the thermal efficiency of cement kiln equipment. At the same time, replacing N_2 with CO_2 can significantly reduce the amount of thermodynamic NO_x generation [4], and the O_2/CO_2 combustion technology used in cement kiln does not affect the clinker strength [5].

Many scholars have compared the fuel combustion situation in the O_2/CO_2 atmosphere and the O_2/N_2 atmosphere, tested the overall performance [6, 7] and the flame stability [8, 9], and conducted the numerical simulation of the flame structure [10, 11], The result shows that flame propagation and oxygen diffusion are slower in O_2/CO_2 atmosphere regardless of fuel type. Suda *et al.* [12] pointed out that the main reason is that the volumetric specific heat capacity of CO_2 is higher than that of N_2. For pulverized coal, Debo *et al.* [13] found through experimental research that the ignition temperature and burnout temperature of pulverized coal in the O_2/N_2 atmosphere are lower than that in the O_2/CO_2 atmosphere. Zhang *et al.* [14] studied the combustion of pulverized coal in the O_2/CO_2 atmosphere boiler and found that the ignition time of pulverized coal in the O_2/CO_2 atmosphere would be delayed.

Currently, the application of O_2/CO_2 combustion technology in cement kilns mainly remains in the theoretical analysis of technical and economic feasibility [15, 16], as well as small-scale and pilot studies [17]. With the increasing maturity and accuracy of computer numerical simulation technology, the decomposition furnace simulation study can be conducted in O_2/CO_2 atmosphere using CFD simulation technology [18]. Francisco *et al.* [19] and Mario and Bakken [20] verified that modern kiln burners are suitable for oxygen fuel combustion without additional modification by experimental and numerical simulation methods, respectively. In the decomposition furnace, Xu *et al.* [21] conducted a numerical simulation study on the combustion of pulverized coal in the decomposition furnace under the O_2/CO_2 atmosphere. They found that the combustion rate of pulverized coal and the decomposition rate of raw meal in the decomposition furnace under the O_2/CO_2 atmosphere was reduced. Zhang *et al.* [22] found that the O_2/CO_2 combustion technology can significantly reduce the outlet NO_x and does not affect the normal work of the decomposition furnace through a numerical simulation study of O_2/CO_2 combustion in the cement decomposition furnace. However, the aforementioned simulation study on the combustion of O_2/CO_2 in the decomposition furnace needs to include the consideration of the changes in the kinetic parameters of $CaCO_3$ decomposition after substituting N_2 with CO_2. It cannot support the application of this technology in the cement decomposition furnace. An experimental study by Tian *et al.* [23] showed that compared with O_2/N_2 atmosphere, the decomposition reaction time of $CaCO_3$ in the O_2/CO_2 atmosphere was prolonged, while the decomposition rate decreased. In addition, the activation energy and pre-exponential factor were greatly improved. Therefore, to further promote the application of O_2/CO_2 combustion technology in the decomposition furnace, the effects of the changes concerning the kinetic parameters of $CaCO_3$ decomposition in the O_2/CO_2 atmosphere should be further explored.

This research is based on the CFD numerical simulation approach and the widely used commercial software FLUENT based on verifying the pulverized coal coupled air combustion model and referring to the variations of the kinetic decomposition parameters of calcium carbonate in an O_2/CO_2 atmosphere. The effect of pulverized coal coupling O_2/CO_2 combustion technology in decomposition furnaces was analyzed and compared, providing theoretical support for promoting O_2/CO_2 combustion technology in decomposition furnaces.

Geometric model and boundary condition

Model introduction

This research uses a CFD numerical simulation analysis based on the actual 3500 tonne per day cement decomposition furnace operating at a cement plant. The decomposition

furnace model is TTF type, it contains two shrinkage regions and three spray regions, which provides the benefits of a powerful reflux impact and longer spray times, the high temperature zone in the middle of the combustion zone can be created by the feeding method of separating the upper and lower feeding points, which can significantly improve the combustion speed of pulverized coal. Figure 1 illustrates the geometric model. The height of the body of the decomposition furnace is 45.68 meters, while the effective interior diameter is 3.5 meters. It consists of the vertebral body, the primary combustion chamber, the middle portion, the top portion of the decomposition furnace, and the shrinkage port. The tertiary air duct is distributed symmetrically on both sides of the bottom of the main combustion chamber, and the four pulverized coal tubes are distributed uniformly above the tertiary air duct. The raw meal is decomposed in a graded manner. The raw meal feeding points are located above the pulverized coal burner and in the center of the decomposition furnace, with two in each tier and four in total. The flue gas created in the cement rotary kiln enters the decomposition furnace from the bottom of the lower vertebral body and escapes through the higher outlet.

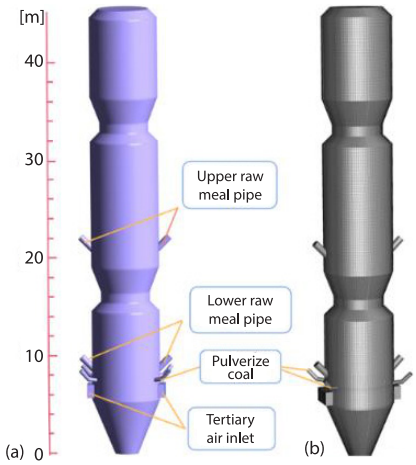

Figure 1. The TTF decomposition furnace structure and mesh

The ANSYS ICEM was used to generate the structured hexahedral grid, and some regions were encrypted to improve simulation accuracy. The total number of created grids was 2217 k. The resulting grid was dense, and no bad grids were produced. The minimal orthogonal quality was 0.72, and the minimum Angle was 45°, satisfying the conditions for calculation precision and calculation time.

Mesh independence

To explore the influence of the number of grids on the simulation results. The outlet temperature of the decomposition furnace in a typical air atmosphere was selected as the research parameter for grid independence verification. The setting of these meshes is listed in tab. 1. We compared the grid number with the decomposition furnace outlet temperature, and the comparison results are shown in fig. 2, when the grid number exceeds 1132 k, the temperature at the decomposition furnace outlet changes

Table 1. Parameter setting of grid refinement study

Grid group	Normalized grid spacing	Outlet temperature	Element number
1	0.6	1070.28	90 k
2	0.2	1120.76	620 k
3	0.16	1132.09	1132 k
4	0.125	1135.54	2217 k
5	0.1	1136.23	4266 k

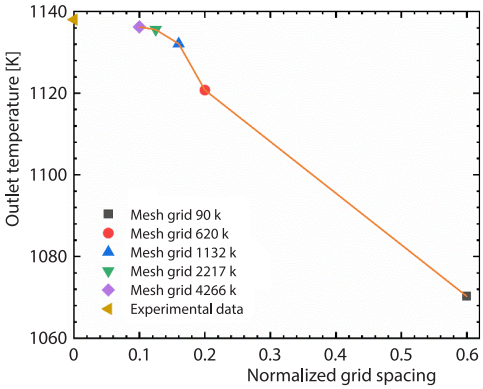

Figure 2. Comparison of outlet temperature among different densities of grid mesh

minimally, and the error with the measured value is within a reasonable range. Thus the grid number 2217 k is selected for this simulation study.

Boundary conditions

The boundary conditions necessary for the calculation are set according to the collected data in the test conditions, and the velocity inlet boundary conditions are utilized for both the flue gas inlet and the tertiary air inlet. The flue gas inlet velocity is 36 m/s, and the tertiary air inlet velocity is 31 m/s. The decomposition furnace outlet boundary condition is pressure outlet, and the pressure value is –1250 Pa. Raw meal and pulverized coal are both imported mass-flow inlets. The Ultimate analysis and proximate analysis of pulverized coal are depicted in tab. 2. In contrast, the composition analysis of raw meals is illustrated in tab. 3, and the mass-flow and average temperature of coal powder and calcium carbonate inlet are depicted in tab. 4. The decomposition furnace is divided into several regions, and the corresponding wall surface temperature is set with the measured temperatures of the various areas. The other positions of the furnace body are selected as the wall surface, and the boundary condition of the wall surface is set as the constant temperature boundary.

Table 2. Proximate and ultimate analyses of pulverized coal

Ultimate analysis					Proximate analysis				$Q_{gr.ad}$ [MJkg^{-1}]
C_{ad}	H_{ad}	O_{ad}	N_{ad}	S_{ad}	FC_{ad}	V_{ad}	A_{ad}	M_{ad}	
60.5	4.03	18.34	1.04	0.26	53.49	30.68	11.69	4.14	26.9

Table 3. Raw meal compositions [%]

Loss*	SiO_2	Al_2O_3	Fe_2O_3	CaO	MgO
36.74	12.56	3.69	2.22	43.41	1.38

* Loss represents the burning loss of raw meal, characterize the percentage of gaseous products (such as H_2O, CO_2, *etc*.) and organic matter content in the total amount of raw meal.

Table 4. Mass-flow and temperature of coal and $CaCO_3$

Parameter	Coal	$CaCO_3$	
		Upper	Lower
Mass-flow [kgs^{-1}]	0.95	20	14.6
Temperature [K]	331	1043	1043

This study compares the O_2/CO_2 atmosphere with the O_2/N_2 atmosphere to better understand the combustion changes of the decomposition furnace under the O_2/CO_2 atmosphere. Compared with the O_2/N_2 atmosphere, only the tertiary air, coal supply air, and N_2 in the flue gas inlet in the standard air atmosphere are replaced by CO_2 in the O_2/CO_2 atmosphere, and the other boundary conditions remain unchanged. Under an O_2/N_2 atmosphere, each component's volume concentration in the tertiary air and pulverized coal inlet gas is 21% O_2 and 79% N_2. Each component's volume concentration in the flue gas inlet gas is 12.7% CO_2, 2.8% O_2, 0.1% CO, and 84.4% N_2. Under an O_2/CO_2 atmosphere, each component's volume concentration in the tertiary air and pulverized coal inlet gas is 21% O_2 and 79% CO_2. In comparison, each component's volume concentration in the flue gas inlet gas is 97.1% CO_2, 2.8% O_2, and 0.1% CO.

Model selection and numerical solution method

Turbulence governing equation

The gas-phase turbulence model adopted the Realizable k-ε [24] model, which is suitable for the decomposition furnace.

Discrete phase model

The discrete phase model model was utilized to solve the particle phase's motion trajectory in the decomposition furnace. The pulverized coal particles were assumed to be spherical, and the particle size was determined using the Rosin-Rammler distribution. The maximum particle size of coal dust is 90 μm, the minimum particle size is 50 μm, and the average particle size is 60 μm. The effect of turbulence on particles is considered. A particle phase random orbit model is established to track the discrete phase, and 23000 coal powder particles are tracked.

In the decomposition furnace, the finite-rate/eddy-dissipation model in the species transport model was utilized for the combustion of pulverized coal and the decomposition of calcium carbonate. The explosion of pulverized coal typically occurs in two-stages: volatile separation and explosion have been assumed to appear first in the coal-combustion process, followed by the eruption of char. The two competing rates model was used for volatile combustion. When the volatile combustion is complete, the remaining coke is reacted, and the reaction rate is controlled by the kinetic/diffusion model chosen. The pulverized coal oxidation reaction is:

$$C_{0.57}H_{3.90}O_{1.12}N_{O.OO726}S_{0.0079} \rightarrow 0.57CO+1.95H_2O+0.0363N_2+0.0079SO_2 \quad (1)$$

$$CO+0.5O_2 \rightarrow CO_2 \quad (2)$$

For the raw meal decomposition study of the decomposition furnace, the raw meal is approximately regarded as $CaCO_3$, and the species transport model is utilized to simulate the decomposition process. The decomposition reaction of $CaCO_3$:

$$CaCO_3 \rightarrow CaO+CO_2 \quad (3)$$

In an O_2/CO_2 atmosphere, the kinetic parameters of $CaCO_3$ decay differ from those in an O_2/N_2 atmosphere. Due to the sluggish diffusion speed of CO_2 created by the decomposition of $CaCO_3$ at high partial pressures of CO_2, which hinders other decomposition reactions and the decay of $CaCO_3$, its pre-exponential factor and activation energy are enhanced proportionally. Table 5 summarizes the kinetic parameters from eqs. (1)-(3).

Table 5. Kinetic parameters of the reactions

Reactant	A	E [Jkmol^{-1}]	Reaction orders
Volatile	$2.119 \cdot 10^{11}$	$2.027 \cdot 10^{8}$	$[\text{volatile}]^{0.2}[O_2]^{1.3}$
CO	$2.239 \cdot 10^{12}$	$1.7 \cdot 10^{8}$	$[CO]^{1}[O_2]^{0.25}$
O_2/N_2 $CaCO_3$	$1.0 \cdot 10^{9}$	$1.95 \cdot 10^{8}$	CO_2 dominant
O_2/CO_2 $CaCO_3$	$3.16 \cdot 10^{31}$	$7.801 \cdot 10^{8}$	CO_2 dominant

The NO_x generating model

The NO_x generation is also an essential generation of understanding pulverized coal combustion. In general, the burst of pulverized coal produces three types of NO_x: thermal NO_x, fuel NO_x, and prompt NO_x. Due to the minimal fraction of prompt NO_x in the pulverized coal combustion process, only thermal NO_x and fuel NO_x are discussed in this paper. The software

Fluent uses post-processing to calculate NO_x so that NO_x generation is influenced by the combustion calculation results [25]. The main reactions of thermal NO_x:

$$O + N_2 \rightleftharpoons N + NO \tag{4}$$

$$N + O_2 \rightleftharpoons O + NO \tag{5}$$

$$N + OH \rightleftharpoons H + NO \tag{6}$$

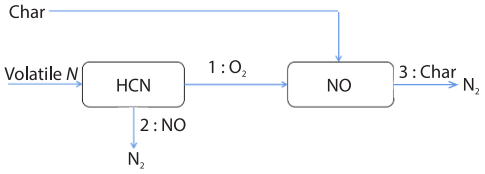

Figure 3. Fuel NO_x formation path

With a complex generation mechanism, fuel NO_x accounts for a significant share of the total NO_x. Figure 3 shows the generation of fuel NO_x [26]. It is hypothesized that N in the fuel is distributed between volatiles and coke, that N in volatiles is converted to NO via the reaction intermediate HCN, and that some unreacted HCN is employed as a reducing agent to convert NO to N_2. N in a coke can be restored immediately to NO.

Radiation model

The P1 radiation model is utilized to calculate the radiation heat transfer between the particle and gas phases. The P1 model is ideal for calculating the heat transfer between the gas and particles in a decomposition furnace due to its small calculation volume and rapid calculation speed. The gas phase absorption coefficient is calculated using the WSGGM model. The parameters used for traditional WSGGM must be changed in the O_2/CO_2 atmosphere due to the high CO_2 partial pressure to accurately replicate the O_2/CO_2 combustion gas radiation [27, 28].

Numerical solution

The finite volume method is used to discretize the continuous phase control equation. The calculation process adopts the SIMPLE algorithm of pressure and velocity coupling. The discrete format pressure is selected as PRESTO! The others use a second-order upwind discrete format. Using TDMA iterative solution, the continuity and energy equation residuals are less than 10^{-6}, and the rest of the residual is less than 10^{-3} as convergence criteria. For the coupling of the continuous phase and particle phase, Solving the constant phase first and then adding a discrete phase is adopted for the coupling of the continuous phase and particle phase.

Numerical simulation results analysis

Verification of the numerical simulation results

In order to verify the reliability of the simulation results, we compared the measured data with the main parameters of the decomposition furnace outlet under the O_2/N_2 conditions. As shown in tab. 6, within 5% are the relative errors of the decomposition furnace outlet temperature and the raw meal decomposition rate under the actual O_2/N_2 conditions, indicating that the selected numerical model is reliable. Shown in fig. 4 are the gas phase composition and measured values at the outlet of the decomposition furnace under O_2/N_2 working con-

Table 6. Comparison of simulation and measured values

Parameter	O_2/N_2	Measured values
Outlet temperature	1132 K	1154 K
Raw meal decomposition rate	95.9%	92.3%

ditions, in which the simulated value of each gas concentration at the outlet of the decomposition furnace is close to the measured value. It indicates that the simulation results meet the requirements of the actual working condition.

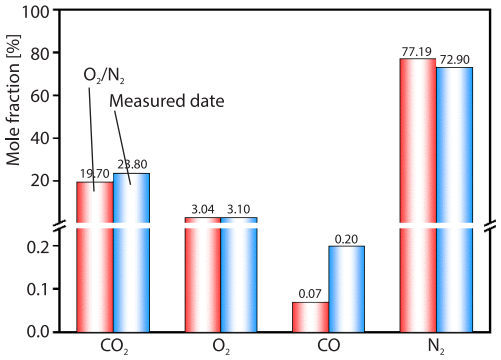

Figure 4. Comparison of simulation and field test at the outlet gas phase composition

Velocity distribution

As shown in figs. 5(a) and 5(b), a good symmetry is observed among the velocity distribution in the decomposition furnace under the two working conditions. Further, the presence of a reflux zone in the bottom vertebral body and the middle part of the decomposition furnace is beneficial to prolong the residence time of the pulverized coal in the furnace and to mix with the raw meal thoroughly. At the same time, the velocity of the air-flow through the shrinking mouth of the decomposition furnace increases remarkably and produces the three ejection effects. Therefore, the heat exchange between the material and the air-flow is strengthened. It is favorable to improve the burning rate of pulverized coal. In addition, by comparison, the velocity distributions under the two working conditions were the same. Meanwhile, the difference between the two is primarily reflected in the size of the reflux area. The main reason is the variation of the pulverized coal combustion and the decomposition of raw meals under the O_2/CO_2 atmosphere.

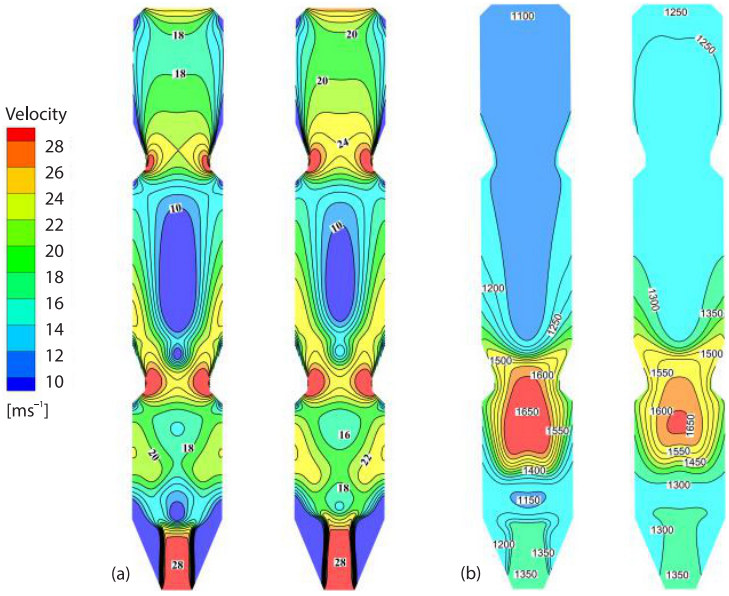

Figure 5. Velocity contours and temperature contours under O_2/N_2 and O_2/CO_2 atmosphere; (a) velocity contours and (b) temperature contours

Temperature distribution

According to the temperature cloud map in figs. 5(c) and 5(d), the decomposition furnace temperature increases and then decreases from the bottom to the top in both conditions. In the first section of the main body, the pulverized coal under high temperature cracking combustion released a large amount of heat and produced a local high temperature area. In the second section main body, as the heat release rate of pulverized coal combustion decreases, $CaCO_3$ decomposes and absorbs heat in a large amount. The temperature in the furnace gradually dropped with a *V*-shaped distribution. When it reached the outlet of the decomposition furnace, the temperature gradually tended to be stable. In addition, by comparing the temperature cloud maps of the two working conditions, it can be seen that the high temperature region in the upper part of the lower raw meal tube in the O_2/CO_2 atmosphere is reduced compared with O_2/N_2 atmosphere. To describe this phenomenon more clearly, we selected the cross-section cloud images at 11 m, 12 m, and 13 m of the primary combustion zone of the decomposition furnace for comparison, as shown in fig. 6. Line A represents the O_2/N_2 atmosphere, and Line B stands for the O_2/CO_2 atmosphere. The comparison shows that at the same position in the main combustion area, the high temperature area of the O_2/CO_2 atmosphere is significantly reduced, and the temperature distribution is more uniform. The main reason is that the combustion capacity of pulverized coal deteriorates under the O_2/CO_2 atmosphere. At the same time, the CO_2 molecules are more radiant and have a more uniform temperature distribution compared with the N_2 molecule. It can also be seen from the temperature cloud map in figs. 5(c) and 5(d) that the temperature keeps increasing from the upper raw meal tube to the outlet of the decomposition furnace under the O_2/CO_2 atmosphere compared with the O_2/N_2 atmosphere, mainly because of the high concentration of CO_2 in the stove under O_2/CO_2 atmosphere inhibits the decomposition of $CaCO_3$. It results in a decrease in the total heat absorbed by the deterioration of the raw meal and an increase in the temperature in the furnace.

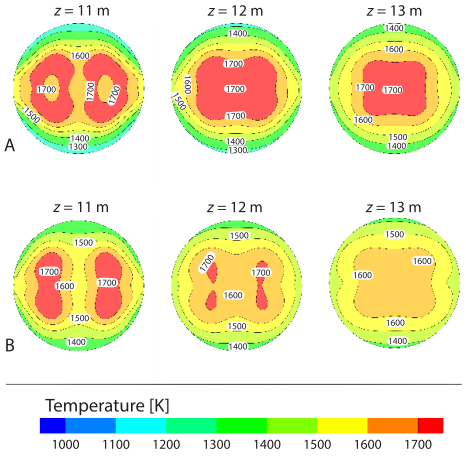

Figure 6. The decomposition furnace z section 11 m, 12 m, and 13 m temperature contour

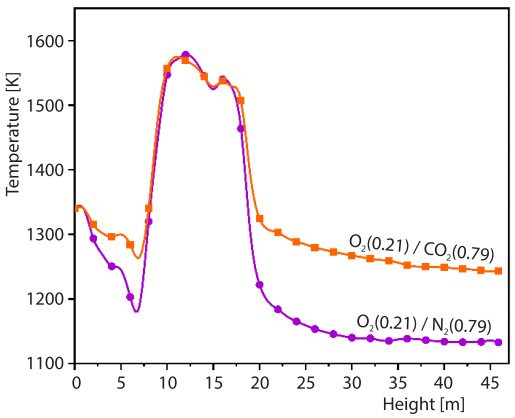

Figure 7. The average cross-sectional temperature along the decomposition furnace

The average temperature of the decomposition furnace section is shown in fig. 7. The temperature in the O_2/CO_2 atmosphere, except the central combustion zone, is higher than O_2/N_2 atmosphere because the high CO_2 partial pressure suppresses the decomposition of $CaCO_3$. The average temperature of the outlet section of the decomposition furnace is 1243 K, which is 111 K more elevated than 1132 K in the O_2/N_2 atmosphere.

The CO and CO_2 distribution

From the results in figs. 8(a) and 8(b), the decomposition furnaces CO are divided into two parts. One is the small amount of CO carried by the kiln tail flue gas itself, which forms a small area in the inlet. The second is the CO produced by incomplete combustion of pulverized coal in the primary combustion zone, including a reduction zone with higher concentration. Under the action of tertiary air, the previously mentioned two react quickly with oxygen. They are converted into CO_2, resulting in the continuous upward consumption of CO with the air-flow until the CO at the outlet of the decomposition furnace is wholly consumed. Compared with the two working conditions, the maximum local concentration of CO in the O_2/N_2 atmosphere is 0.31%, and CO in O_2/CO_2 atmosphere is 0.4%. It indicates that the pulverized coal is almost completely burned. In the O_2/CO_2 atmosphere, the CO content in the flue gas inlet and the main combustion area has increased. It is consistent with the results of Tan *et al.* [29] on a 0.3 MW vertical combustor research facility. The main reason is that the high concentration of CO_2 can inhibit the synthesis of CO and reduce the conversion rate of CO, thus improving its content.

As seen from figs. 8(c) and 8(d), the CO_2 entering from the bottom flue gas inlet of the decomposition furnace under the O_2/N_2 atmosphere gradually increases along the decomposition furnace from bottom to top, with a slight decrease in the concentration at the tertiary air position. The main reason is that the added attention of air is diluted. And in the primary combustion area, the CO_2 concentration gradually increases due to the combustion of pulverized coal and the release of CO_2 from the decomposition of calcium carbonate. Specifically, the enriched CO_2 concentration at the outlet of the decomposition furnace was 19.7%. Besides, in the O_2/CO_2 atmosphere, the CO_2 concentration at the bottom flue gas inlet was as high as 97.1%. It dramatically changes the distribution of CO_2 concentration. At the tertiary air location, the CO_2 concentration is diluted and reduced due to the addition of an O_2/CO_2 atmosphere. In addition, two low concentration zones are created due to the inhibition of $CaCO_3$ decomposition by the high CO_2 atmosphere near the upper and lower raw metal pipes. Two V-shaped areas also appear in the corresponding fig. 9. After that, the CO_2 concentration was gradually enriched and stabilized, reaching 75.4% at the outlet of the decomposition furnace.

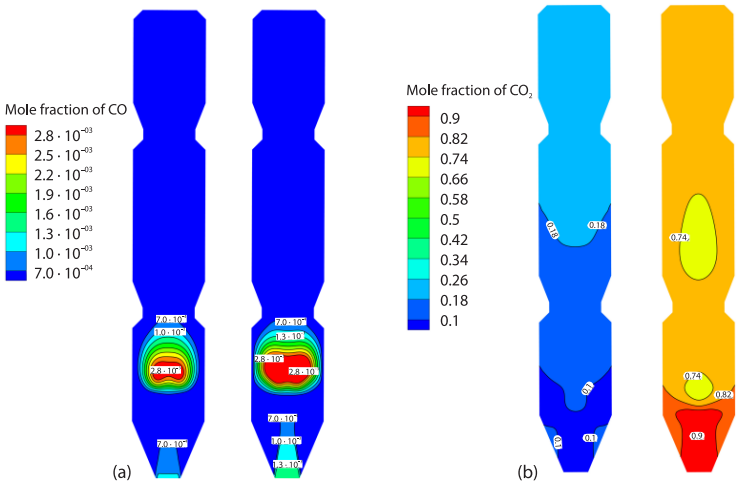

Figure 8. The CO and CO_2 mole fraction distributions under O_2/N_2 and O_2/CO_2 atmosphere; (a) CO mole fraction and (b) CO_2 mole fraction

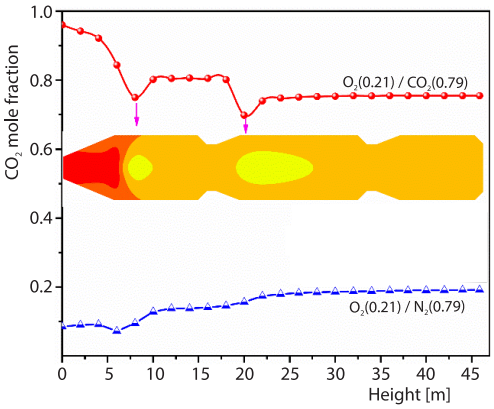

Figure 9. Average cross-sectional CO_2 mole fraction along the decomposition furnace

The $CaCO_3$ and CaO distribution

According to figs. 10(a) and 10(b), combined with fig. 11, the trends of $CaCO_3$ concentration in the two working conditions are relatively consistent. In both cases, the height direction is first rising, then falling, followed by rising, and finally falling again. The two elevated positions correspond to the raw meal entrance, and the second peak of the curve is higher because of the more extensive feed of the upper raw meal. First, after entering the decomposition furnace, $CaCO_3$ decomposes rapidly due to the high temperature environment generated by the pulverized coal combustion. It has been entirely spoiled by the time it reaches the entrance of the upper raw meal. Subsequently,

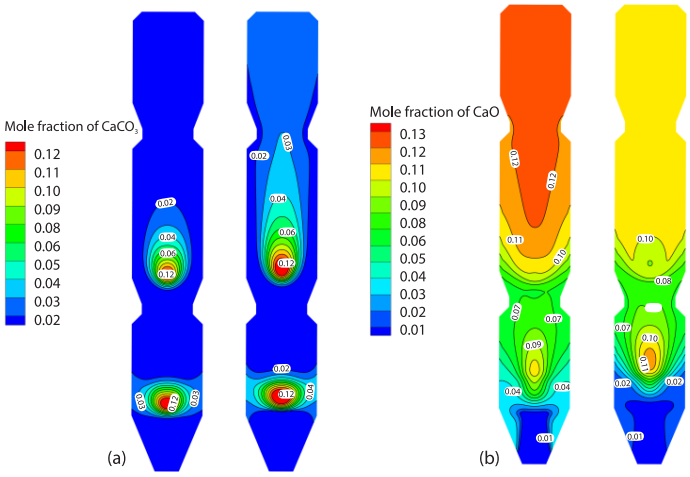

Figure 10. The $CaCO_3$ and CaO mole fraction distributions under O_2/N_2 and O_2/CO_2 atmosphere; (a) $CaCO_3$ mole fraction and (b) CaO mole fraction

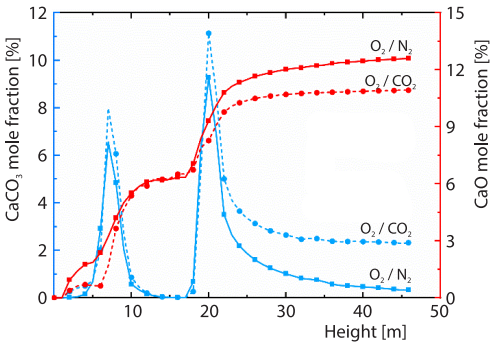

Figure 11. Average cross-sectional $CaCO_3$ and CaO mole fraction along the decomposition furnace

after feeding the raw meal into the upper raw meal pipe, the $CaCO_3$ mole material fraction climbs up rapidly, decreases after decomposition, and stabilizes. Comparing the two working conditions, the $CaCO_3$ concentration peak of the upper and lower raw meal pipes in the O_2/CO_2 atmosphere is higher than that of the O_2/N_2 atmosphere. The main reason is that the O_2/CO_2 atmosphere suppresses $CaCO_3$ decomposition some extent, and the added $CaCO_3$ is not decomposed in time. This results in a large local $CaCO_3$ concentration in the O_2/CO_2 atmo-

sphere. In addition the peak value, the variation of $CaCO_3$ concentration at 0-6 m and 8-20 m of the decomposition furnace are similar under the two working conditions. At 20 m from the outlet, the $CaCO_3$ concentration in O_2/CO_2 atmosphere is higher than that in O_2/N_2 atmosphere. The main reason is that not only is temperature dependent is the decomposition, but also subject to the partial pressure of CO_2. In the case of the dominant role of temperature in the main combustion zone, $CaCO_3$ can decompose entirely in both atmospheres at a suitable temperature. However, after the main combustion zone, the temperature of the decomposition furnace decreases due to the addition of raw meal in the upper raw pipe, and the partial pressure of CO_2 plays a dominant role in the decomposition of $CaCO_3$. The high partial pressure of CO_2 in the O_2/CO_2 atmosphere is not conducive to the further decomposition of $CaCO_3$. This eventually leads to higher concentrations of $CaCO_3$ in the O_2/CO_2 atmosphere than in the normal air atmosphere after the main combustion zone. The calculated mass-flow rates of $CaCO_3$ at the outlet of O_2/N_2 and O_2/CO_2 are 2.9 kgs and 12.3 kgs., respectively, the corresponding decomposition rates are 95.9% and 82.1%. Compared with the O_2/N_2 atmosphere, the decomposition rate of $CaCO_3$ under the O_2/CO_2 atmosphere can be improved by optimizing the process parameters.

According to the results of figs. 10(c) and 10(d), combined with fig. 11, the trend of CaO concentration is just opposite to that of $CaCO_3$, showing a gradual enrichment from bottom to top. When the concentration of $CaCO_3$ attention near the upper and lower raw meal tubes decreases significantly, the growth rate of CaO is the fastest. As the decomposition rate of $CaCO_3$ in the upper furnace body drops, the growth rate of CaO becomes smaller and stabilizes at the outlet of the decomposition furnace. Compared with the two working conditions, it can be found that the enriched CaO content at the decomposition furnace outlet is reduced in the O_2/CO_2 atmosphere, down from 12.6% in the typical air atmosphere to 10.9%.

The O_2 and NO_x distribution

According to figs. 12(a) and 12(b), under the O_2/N_2 atmosphere, the O_2 carried by the tertiary air has the highest concentration in the decomposition furnace primary combustion area was about 8~14%. Due to the decisive vortex flow action of tertiary air, the high concentration of O_2 region is distributed in the near-wall area of the tertiary air. In contrast, the central area

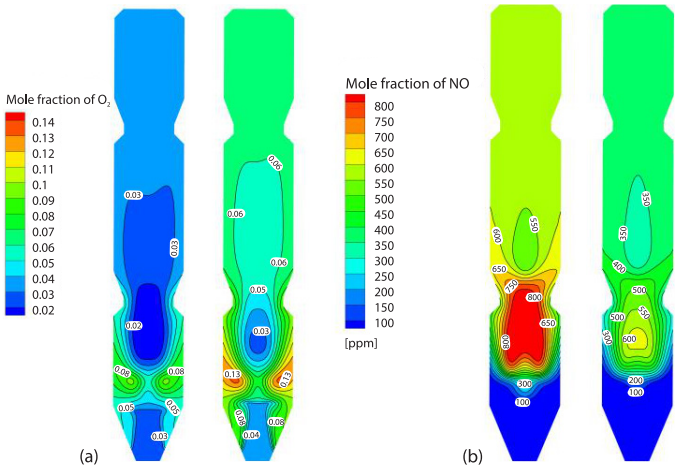

Figure 12. The O_2 mole fraction distributions and NO_x contours under O_2/N_2 and O_2/CO_2 atmosphere; (a) O_2 mole fraction and (b) NO_x contours

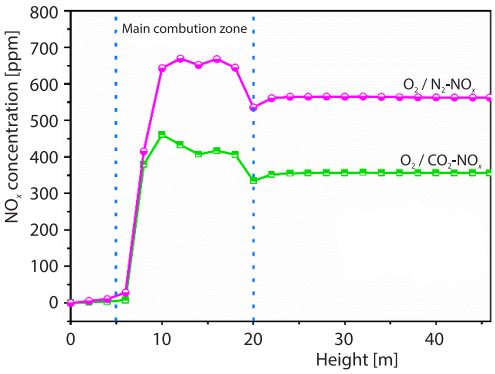

Figure 13. Average cross-sectional NO concentration along the decomposition furnace

concentration is negligible. With the combustion of pulverized coal, O_2 is rapidly consumed, and the concentration gradually decreases. Concentration at the outlet of the decomposition furnace was only 3.04%, which is consistent with the measured value. Compared with the O_2 concentration in O_2/CO_2 atmosphere, the O_2 content in the primary combustion region in the O_2/CO_2 atmosphere was about 9~17%. It is mainly because the high CO_2 concentration in O_2/CO_2 atmosphere deteriorates the combustibility of pulverized coal and reduces the O_2 consumption. Under this influence, along the direction of furnace height, the O_2 concentration of the whole decomposition furnace in the O_2/CO_2 atmosphere increased to 6.05% at the outlet of the decomposition furnace, which is twice as high as in the O_2/N_2 atmosphere.

As can be seen from figs. 12(c) and 12(d), the NO_x content in the primary combustion area increases rapidly under the O_2/N_2 atmosphere. It forms a high concentration NO_x area corresponding to the high temperature area in fig. 13. The local maximum NO_x concentration can reach 670 ppm (equivalent to 738 mg/m^3), primarily due to the rapid generation of thermal NO_x and fuel NO_x in the main combustion area. In the vicinity of the upper raw meal tube, the decomposition furnace temperature is reduced due to the addition of many raw meals. Also, the NO_x content decreases to a certain extent until it stabilizes at the decomposition furnace outlet with a value of about 562 ppm (equivalent to 619 mg/m^3). Under the O_2/CO_2 atmosphere, there is almost no thermal NO_x generation because no N_2 is introduced. At the same time, the high concentration of NO_x in the primary combustion zone is significantly reduced because the high CO_2 atmosphere increases the mass fraction of CO in the decomposition furnace. Reducing CO has an inhibitory effect on the generation of fuel NO_x. After the gradual dilution of the updraft, the concentration of NO_x at the outlet of the decomposition furnace is stabilized at 355 ppm (equivalent to 391 mg/m^3). Remarkably, compared with the O_2/N_2 atmosphere, the NO_x at the outlet of the decomposition furnace is reduced by 37%.

Conciusions

For the TTF decomposition furnace, the coal powder combustion and calcium carbonate decomposition under O_2/N_2 and O_2/CO_2 atmosphere were investigated and compared, and the mechanism was studied, are as follows.

- The results show that a high CO_2 atmosphere dramatically influences the kinetic parameters of $CaCO_3$ decomposition with a corresponding increase in pre-exponential factor and activation energy compared with O_2/N_2 combustion-supporting mode. As a result, the outlet temperature of the decomposition furnace in the O_2/CO_2 atmosphere was increased by 111 K, and the oxygen content was doubled. At the same time, the decomposition rate of raw meals in the decomposition furnace decreased from 95.9-82.1% under the O_2/CO_2 atmosphere. Given this, optimizing the process parameters to improve the decomposition rate of $CaCO_3$ under the O_2/CO_2 atmosphere is necessary.
- Under the O_2/CO_2 atmosphere, the velocity field in the furnace did not change significantly. Meanwhile, with the strong radiation capacity of CO_2 molecules, the temperature distribu-

tion in the high temperature zone in the furnace was more uniform, and the range of the high temperature area was narrowed. It is beneficial to improve the clinker strength and reduce the fume volume. In addition, the high concentration of CO_2 at the outlet can be recovered and collected, which is conducive to the reduction of CO_2 emission.

- The high CO_2 partial pressure significantly reduced the thermal NO_x in the decomposition furnace. Compared with the O_2/N_2 atmosphere, the high concentration of NO_x area was significantly reduced in the primary combustion area under the O_2/CO_2 atmosphere, and the concentration of NO_x at the decomposition furnace was reduced from 619-391 mg/m^3. The NO*x* at the outlet of the decomposition furnace was decreased by 37%.

References

[1] Liu, Y., Kao, H., Numerical Simulation of Urea Based SNCR Process in a Trinal-Sprayed Precalciner, *Journal of Renewable Materials*, *9* (2021), 2, pp. 269-294
[2] Li, H., *et al.*, Impurity Impacts on the Purification Process in Oxy-Fuel Combustion Based CO_2 Capture and Storage System, *Applied Energy*, *86* (2009), 2, pp. 202-213
[3] Tu, Y., *et al*., The CFD and Kinetic Modelling Study of Methane MILD Combustion in O_2/N_2, O_2/CO_2 and O_2/H_2O atmospheres, *Applied Energy*, *240* (2019), Apr., pp. 1003-1013
[4] Liu, H., *et al*., Pulverized Coal Combustion in Air and in O_2/CO_2 Mixtures with NO_x Recycle, *Fuel*, *84* (2005), 16, pp. 2109-2115
[5] Zheng, L., *et al*., Phase Evolution, Characterisation, and Performance of Cement Prepared in an Oxy-Fuel Atmosphere, *Faraday Discussions*, *192* (2016), Apr., pp. 113-124
[6] Dally, B. B., *et al*., On the Burning of Sawdust in a MILD Combustion Furnace, *Energy and Fuels*, *24* (2010), 6, pp. 3462-3470
[7] Li, P., *et a*l., The MILD Oxy-Combustion of Gaseous Fuels in A Laboratory-Scale Furnace, *Combustion and Flam*e, *160* (2013), 5, pp. 933-946
[8] Khalil, A. E. E., Gupta, A. K., Flame Fluctuations in Oxy-CO_2-Methane Mixtures in Swirl Assisted Distributed Combustion, *Applied Energy*, *204* (2017), Oct., pp. 303-317
[9] Khalil, A. E. E., Gupta, A. K., The role of CO_2 on Oxy-Colorless Distributed Combustion, *Applied Energy*, *188* (2017), Feb., pp. 466-474
[10] Yaojie, *et al*., Physical and Chemical Effects of CO_2 Addition on CH_4/H_2 Flames on a Jet in Hot Coflow (JHC) Burner, *Energy Plus*, *30* (2016), 2, pp. 1390-1399
[11] ***, Flame Characteristics of CH_4/H_2 on a Jet-in-Hot-Coflow Burner Diluted by N_2, CO_2, and H_2O (2017)
[12] Suda, T., *et al*., Effect of Carbon Dioxide on Flame Propagation of Pulverized Coal Clouds in CO_2/O_2 combustion, *Fuel*, *86* (2007), 12-13, pp. 2008-2015
[13] Debo, L., *et al*., Coal Combustion Characteristics and Kinetics Analysis in O_2/CO_2 Atmosphere, *Journal of Combustion Science and Technology*, *24* (2018), 3, pp. 223-231
[14] Zhang, L., *et al*., The Chemical and Physical Effects of CO_2 on the homogeneous and heterogeneous ignition of the coal particle in O_2/CO_2 Atmospheres, *Proceedings of the Combustion Institute*, *36* (2017), 2, pp. 2113-2121
[15] Rolfe, A., *et al*., Technical and Environmental Study of Calcium Carbonate Looping vs. Oxy-Fuel Options for low CO_2 Emission Cement Plants, *International Journal of Greenhouse Gas Control*, *75* (2018), Aug., pp. 85-97
[16] Plaza, M. G., *et al*., The CO_2 Capture, Use, and Storage in the Cement Industry: State of the Art and Expectations, *Energies*, *13* (2020), 21
[17] Telesca, A., *et al*., Low-CO_2 Cements from Fluidized Bed Process Wastes and Other Industrial by-Products, *Combustion Science and Technology*, *188* (2016), 4-5, pp. 492-503
[18] Granados, D. A., *et al*., Effect of Flue Gas Re-Circulation during Oxy-Fuel Combustion in a Rotary Cement Kiln, Energy, *64* (2014), Jan., pp. 615-625
[19] Carrasco, F., *et a*l., Experimental Investigations of Oxyfuel Burner for Cement Production Application, *Fuel*, *236* (2019), Jan., pp. 608-614
[20] Mario, D., Bakken, J., Study of a Full Scale Oxy-Fuel Cement Rotary Kiln, *International Journal of Greenhouse Gas Control*, *83* (2019), Apr., pp. 166-175
[21] Xu, S., *et al*., Numerical Simulation and Reliability Verification of Pulverized Coal Combustion in Rotary Kiln and Decomposing Furnace under O_2/CO_2 Condition, *Chinese Journal of Environmental Engineering*, *14* (2020), 5, pp. 1311-1319

[22] Leyu, Z., *et al*., Numerical Simulation of O_2/CO_2 Combustion in Large Cement Precalciner, *Scientia Sinica Technologica*, *49* (2019), 9, pp. 1080-1088
[23] Tian, H., *et al*., Study of Kinetic Characteristics of Limestone Decomposition under Different Atmospheres and Heating Conditions, *Journal of Thermal Analysis and Calorimetry*, *130* (2017), 3, pp. 2351-2358
[24] Shih, T., *et al*., A new k-ϵ eddy viscosity model for high reynolds number turbulent flows, *Computers & Fluids*, *24* (1995), 3, pp. 227-238
[25] Lockwood, F., Romomillares, C., Mathematical-Modelling of Fuel – No Emissions from Pf Burners, *Journal of the Institute of Energy*, *65* (1992), 464, pp. 144-152
[26] Xin, C., Yongliang, M., Numerical simulation of Flow and Temperature Field in a Cement Precalciner, *Chinese Journal of Environmental Engineering*, *8* (2014), 10, pp. 4349-4354
[27] Guo, J., *et al*., Experimental and Numerical Investigations on Oxy-Coal Combustion in a 35 MW Large Pilot Boiler, *Fuel*, *187* (2017), Jan., pp. 315-327
[28] Guo, J., *et al*., Numerical investigation on Oxy-Combustion Characteristics of a 200MWe Tangentially Fired Boiler, *Fuel*, *140* (2015), Jan., pp. 660-668
[29] Tan, Y., *et al.*, Combustion Characteristics of Coal in a Mixture of Oxygen and Recycled Flue Gas, *Fuel*, *85* (2006), 4, pp. 507-512

Paper submitted: December 17, 2022
Paper revised: February 28, 2023
Paper accepted: March 1, 2023